

Article

Rational Alloy Design of Niobium-Bearing HSLA Steels

Rami A. Almatani ¹  and Anthony J. DeArdo ^{1,2,*}

¹ The Basic Metals Processing Research Institute, Department of Mechanical Engineering and Materials Science, University of Pittsburgh, Pittsburgh, PA 15261, USA; raa148@pitt.edu

² Finland Distinguished Professor, Department of Mechanical Engineering, University of Oulu, P.O. Box 4200 (Linnanmaa), FIN-90014 Oulu, Finland

* Correspondence: deardo@pitt.edu; Tel.: +1-412-996-6770

Received: 20 February 2020; Accepted: 18 March 2020; Published: 23 March 2020



Abstract: In the 61 years that niobium has been used in commercial steels, it has proven to be beneficial via several properties, such as strength and toughness. Over this time, numerous studies have been performed and papers published showing that both the strength and toughness can be improved with higher Nb additions. Earlier studies have verified this trend for steels containing up to about 0.04 wt.% Nb. Basic studies have shown that the addition of Nb increases the recrystallization-stop temperature, $T_{5\%}$ or T_{nr} . These same studies have shown that with up to about 0.05 wt.% of Nb, the $T_{5\%}$ temperature increases in the range of finish rolling, which is the basis of controlled rolling. These studies also have shown that at very high Nb levels, exceeding approximately 0.06 wt.% Nb, the recrystallization-stop temperature or $T_{5\%}$ can increase into the temperature range of rough rolling, and this could result in insufficient grain refinement and recrystallization during rough rolling. However, the question remains as to how much Nb can be added before the detriments outweigh the benefits. While the benefits are easily observed and discussed, the detriments are not. These detriments at high Nb levels include cost, undissolved Nb particles, weldability issues, higher mill loads and roll wear and the lessening of grain refinement that might otherwise occur during plate rough rolling. This loss of grain refinement is important, since coarse grained microstructures often result in failure in the drop weight tear testing of the plate and pipe. The purpose of this paper is to discuss the practical limits of Nb microalloying in controlled rolled low carbon linepipe steels of gauges ranging from 12 to 25 mm in thickness.

Keywords: HSLA steel; alloy design; grain refinement of austenite; Zener pinning force; recrystallization; Niobium Nb

1. Introduction

It has been over 61 years since the first production heat of a niobium (Nb) bearing HSLA strip steel was commercially produced in 1958 [1,2]. Since that time, microalloying with Nb has been extended to virtually all product classes and forms. Perhaps nowhere has Nb been more beneficial than in linepipe steels for high pressure oil and gas transmission at low temperatures. The contribution of Nb to high strength by grain refinement; solid solution strengthening of the various types of ferrite formed; and further strengthening of the ferrite by precipitation and dislocation-hardening through increased hardenability have all been chronicled in numerous papers and research studies [3–8]. In a similar fashion, the improvement in lowering the ductile-brittle transition temperature (DBTT) through the use of niobium is critically important in pipelines intended for low temperature service [9]. Much of this improvement is caused by the grain refinement of both the austenite during hot rolling, and the grain refinement of the ferrite during transformation upon cooling. Several studies have shown

that strength and toughness can be improved by increasing the level of Nb used, from zero to the conventional 0.03–0.04 wt.%, to very high levels near 0.1% Nb [10,11]. However, there are detriments beyond cost to the use of Nb, especially at higher levels, such as reduced weldability, large undissolved particles and higher mill loads.

When a 25 mm thick plate intended for pipe applications is hot rolled on a modern 5 m plate mill, it does so in three stages after slab reheating: rough rolling, finish rolling and accelerated cooling. For example, after reheating at 1200 °C, a continuously cast slab of 200 mm thickness might be rolled to 75 mm transfer bar in the roughing mill at temperature from 1150–1050 °C. The bar is then transported to the finishing stands, where it is further rolled to the final gauge of 25 mm at temperatures ranging from below 900 to 750 °C. Because of the large width and potentially high mill loads, the rough rolling and finishing rolling take place in numerous, light passes, often between 10 and 15 passes in each case, with pass reductions between 10–15% each in the roughing mill, and 5–10% each in the finishing mill. Since these are reversing mills, the interpass times can range from 10–30 s depending on conditions.

After final rolling, the plate is water spray cooled at about 30 °C/s to the water end temperature (WET) which is dictated by the continuous cooling transformation (CCT) diagram, the cooling path and the required microstructure and properties [9]. The WET for achieving ferrite–pearlite microstructures in steels of high hardenability, i.e., CE_{II} over 0.40, is in the range of 600–650 °C. When a bainitic ferrite microstructure is desired, a WET near 450–550 °C would be used. For even higher strengths, requiring martensite, a WET around 300 °C would be used. Normally, the steels are air cooled to room temperature from the WET.

The microstructure of austenite during hot rolling of Nb-bearing HSLA steels is believed to behave according to Figure 1 [12]. For a given strain, above $T_{95\%}$, austenite grains are repeatedly recrystallized and grain refined (complete recrystallization; RXN), while below $T_{5\%}$, the austenite grains are unrecrystallized and pancaked. These critical temperatures are themselves dependent on the content of Nb of steels and increase with higher Nb levels, as shown schematically in the red-dashed curves in Figure 1.

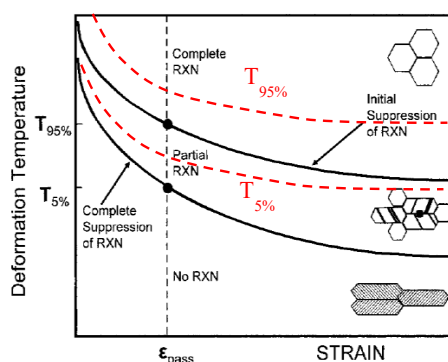


Figure 1. Schematic diagram of the resulting austenite microstructures from different deformation conditions, after reference [12]. $T_{5\%}$ and $T_{95\%}$ are temperatures for 5% and 95% recrystallization, respectively.

The hot processing of Nb steels is based on most of the Nb being in solution in the austenite during slab reheating and rough rolling, and some of the dissolved Nb being reprecipitated as strain-induced precipitate in deformed austenite during finish rolling. The nose of the C-curve for this precipitation in austenite is around 900 °C for 0.04 wt.% Nb, but is raised to 950 °C or higher at larger levels of Nb [3,13]. As mentioned above, studies of the recrystallization-stop-temperature, $T_{5\%}$ or T_{nr} , indicate that this temperature increases with Nb content and can reach or exceed 1050 °C in typical pipe steels containing 0.1% Nb [6,14]. Since the last roughing passes occur in this temperature range, it is quite possible that there might be strain-induced precipitation of NbC, even in the late roughing passes. Since the grain refinement expected during roughing requires multiple static recrystallization events in

the interpass times, perhaps complete recrystallization may not occur by the exit of the roughing mill. Therefore, there might be consequences for the grain refinement needed during rough rolling when the bulk Nb level is too high. For example, this lack of sufficient grain refinement is important, since coarse grained microstructures often result in failure in drop weight tear testing of plate and pipe.

Whether static recrystallization occurs or not depends on the comparison of the driving force for static recrystallization and the retarding Zener pinning force caused by the interaction of the moving austenite boundaries with particles formed earlier on the defect structure of the deformed austenite in the roll gap; these defects include grain and subgrain boundaries and deformation bands [15].

The potential for strain-induced precipitation of NbC or NbCN will depend on the bulk composition of the steel, the relevant solubility products for NbC or NbCN in austenite and the applicable rolling practice. The carbon content will be governed by the final strength needed in the final pipe, which can be X50–60 for ferrite–pearlite (F–P) microstructures, X70–100 for bainitic microstructures and X120 and above for martensitic microstructures [16,17]. While changes in %C have only a slight influence on the strength of F–P steels, they can have dramatic effects on the strength of bainite or martensite found in direct quenched steels. Therefore, the carbon content can be expected to influence both the strength of the plate or pipe through hardenability effects, and the toughness through its effect on the precipitation in austenite and the control of grain size.

The effect of hot rolling on toughness or lowering the DBTT, through grain refinement of the prior austenite grain size (PAGS), is the result of two sequential events. The first is the combination of the elimination of both the remaining as-cast structure and the large grain size that result from slab reheating. These occur during the repeated static recrystallization that takes place between the rough rolling passes that arise when the pass strains happen above the $T_{95\%}$ temperature. This leads grain refinement during multiple waves of recrystallization, where the PAGS might be reduced from 300 μm to 50 μm going into the finishing passes where pancaking occurs.

Since the finishing passes for controlled rolling are usually considered to occur below the $T_{5\%}$ or recrystallization stop temperature, normally about 900 °C in a steel containing 0.04% Nb, the final austenite will be heavily strained, elongated or pancaked [18]. This austenite is highly deformed with high strength and contains numerous crystallographic defects, such as deformation twins, deformation bands, subgrain boundaries and elongated grain boundaries. These near-planar crystalline defects contribute to what is called the S_v value, an index used to judge the effectiveness of a given rolling process in thermomechanical processing (TMP) [19]. In low hardenability or slowly cooled F–P steels, the nucleation of polygonal ferrite occurs on the S_v , where the high density of high angle ferrite grain boundaries resulting from ferrite grain refinement can act as crack arresters for potentially growing cleavage cracks. In higher hardenability or faster cooled steels, the defects themselves can act as cleavage crack arresters in bainitic or martensitic steels. In either case, these near planar defects can act as sites for crack arresters for the growth of cleavage cracks; hence, lowering the DBTT.

To investigate the rough rolling process, the possibility of strain-induced precipitate was explored in this research in the temperature range for rough rolling, i.e., 1150–1000 °C, for a series of steels with two carbon levels: a conventional one of 0.06 wt.% C and a lower carbon version of 0.03 wt.% C. Three levels of Nb were also studied—0, 0.04 and 0.08 wt.%.

The purpose of the current study was threefold: (i) to determine whether NbC could form during rough rolling and (ii) whether this precipitate might cause less than complete recrystallization during rough rolling, and (iii) therefore, lead to a larger slightly pancaked as-roughed austenite grain size resulting in non-optimum final austenite microstructure prior to transformation. To achieve these goals, two investigations were conducted. The first was a theoretical study of potential strain induced precipitation of NbC in the temperature range in which roughing passes would normally occur in a modern 5 m wide reversing plate mill. This required solubility calculations, the use of the subgrain boundary Zener pinning model and parameters taken from similar, earlier studies [3,18,20,21]. The second was the study of the austenite grain size and shape in quenched specimens after laboratory hot deformation experiments conducted in the temperature range in which rough rolling would normally

occur. It was expected that this research would help answer the question as to whether high Nb steels can be expected to be successfully processed on modern plate mills in a range of strength levels.

2. Research Rationale

2.1. Alloy Design Used in Study

The experimental alloys were chosen to represent a typical linepipe steel, near X100 composition [16]. As mentioned earlier, the carbon and niobium levels were chosen to demonstrate the effects of NbC pinning forces in the temperature range of rough rolling. Figure 2 shows the temperature profile of a modern, 5 m wide reversing plate mill where the end of roughing rolling is approximately at 1050 °C [22].

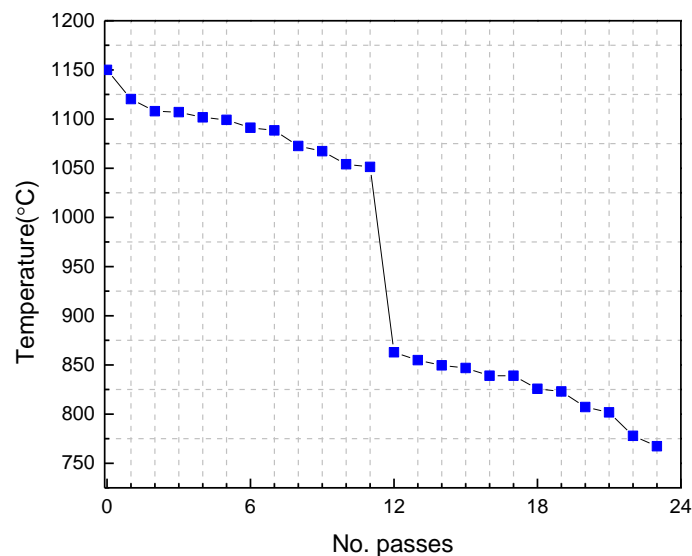


Figure 2. Temperature profile of a modern 5 m wide reversing plate mill, after reference [22].

NbC in solution was calculated using the equilibrium solubility product proposed by Palmiere et al. [20]:

$$\log[\text{Nb}][\text{C}] = 2.06 - \frac{6700}{T} \quad (1)$$

Figure 3 shows the calculated dissolution temperatures of alloys with two Nb levels, namely, 0.04Nb and 0.08Nb, in wt.% while keeping carbon as a constant at 0.06 wt.%. It is clear that all the NbC available in 0.04 wt.% Nb steel will be dissolved at/or close to 1170 °C, while the higher Nb content will not be fully dissolved below a slab reheating temperature of 1265 °C, which indicates more stable precipitates at higher temperatures. It should be noted that this temperature far exceeds the normal reheating temperature of 1150–1200 °C used in practice. The dashed line represents the deviation between the two alloys in terms of soluble NbC; thus, the reheating temperature is not a variable, but is restricted to 1150–1200 °C in practice. Therefore, the question is how much Nb can be dissolved at perhaps 1200 °C. According to Figure 3, all of Nb in the 0.04 steel and 0.55% Nb in the 0.08 steel would be dissolved at 1200 °C. In normal practice with a commercial steel of similar composition containing 0.04Nb, all of the Nb is taken into solution during reheating, and very little if any is reprecipitated during rough rolling. Therefore, recrystallization goes to completion in roughing. However, in the 0.08Nb steel, only 0.055 wt.% Nb is taken into solution and the remaining 0.025 wt.% Nb is left undissolved. The question is: will any of the 0.055 wt.% Nb dissolved in austenite reprecipitate during roughing, and if it does, will it suppress complete recrystallization during roughing? Higher Nb levels

indicate that some precipitates could not be taken into solution based on solubility considerations in the range applicable to the rough rolling process.

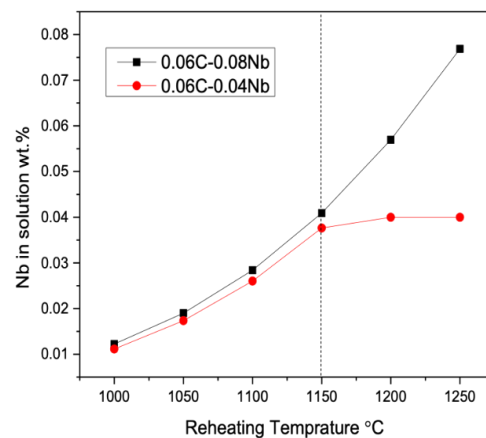


Figure 3. Calculated amount of dissolved Nb at equilibrium as a function of reheating temperature.

2.1.1. Phase I: Theoretical Study

The assumptions made here were that with the addition of Nb into the steel, the $T_{5\%}$ and $T_{95\%}$ temperatures will both be increased [18], and subsequently the processing window above $T_{95\%}$ will be reduced. In addition, the $T_{5\%}$ temperature might be increased to where it enters the later portion of the rough rolling temperature range. Figure 4 shows a schematic of two Nb steels, namely, 0.1Nb and 0.04Nb, in wt.%. For a given strain (i.e., Σn_{passes}) and temperature, and as the temperature decreases, the processing window at the end of roughing for a uniform austenite grain size distribution is reduced in the 0.1Nb steel, below which only partial recrystallization and grain refinement may occur; this is shown in the hatched area above 0.1Nb $T_{95\%}$. On the other hand, the processing window for the 0.04Nb steel to produce a uniform grain size distribution is higher even below 1050 °C, which is here designated as the end of rough rolling temperature.

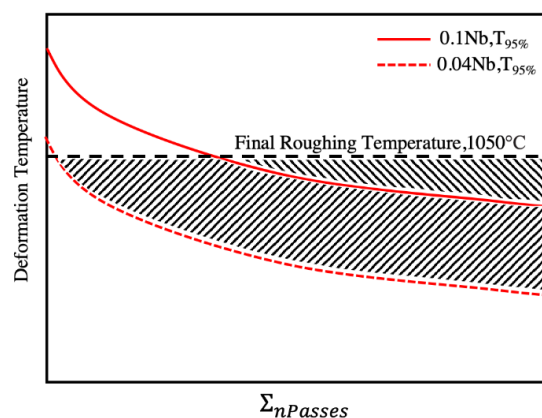


Figure 4. Schematic showing the processing window of high and low Nb steels; hatched areas show the window for which a uniform grain refined austenite microstructure can be obtained by rolling above the respective $T_{95\%}$ temperature.

In the context of hot rolling, the typical value of the recrystallization driving force of austenite subjected to a single low temperature rolling pass is found to be about 22 MPa [12]. This was for 900 °C; at 1100 °C it would be much lower, near 10 MPa. Thus, to retard recrystallization, a necessary pinning force is needed and several models were proposed to calculate the pinning force of precipitates in microalloyed steels as a result of the interaction between precipitates and austenite grain

boundaries [18,23]. However, in this study, as mentioned earlier, the subgrain boundary model [3] was employed to estimate, theoretically, the pinning forces at different deformation temperatures and specifically during roughing passes. The reason for using this model is mainly that NbC particles are not randomly distributed but isolated on the subgrain boundaries of deformed austenite [24,25].

The estimations of pinning forces caused by strain induced precipitation of NbC were calculated using (i) the subgrain boundary model, together with (ii) the volume fractions of NbC estimated for the compositions and temperatures using the equilibrium solubility relation mentioned previously; (iii) particle sizes of NbC observed; and (iv) the dislocation cell sizes observed in the TEM in recovered austenite in earlier similar studies [17,20]. The subgrain boundary pinning force model used was [3]:

$$F = \frac{3\gamma f_v l}{2\pi r^2} \quad (2)$$

where γ is the high angle austenite grain boundary energy, f_v is the volume fraction of precipitates, l is the subgrain size and r is the particle size. The parameters used in this investigation were $\gamma = 0.8 \text{ J/m}^2$, particle size = 2 nm and subgrain size = 0.5 μm ; and f_v can be calculated from the solubility product.

It should be mentioned that the measured volume fractions of NbC for subgrain and grain boundaries were higher than predicted by equilibrium considerations [20]. It appeared that there was a segregation of Nb to the boundaries leading to higher than expected local volume fractions of NbC. This means that the local pinning forces are actually larger than those which would be calculated from equilibrium considerations

Table 1 shows the estimated pinning forces for two alloys, during roughing passes. The results indicate that higher Nb level gives the higher pinning force magnitudes at the end of roughing passes (i.e., 41 MPa at 1050 °C), due to higher volume fraction of NbC to precipitate at lower roughing temperature.

Table 1. NbC pinning force at the respective deformation temperature, MPa.

Deformation Temperature, °C	0.06C,0.08Nb	0.06C,0.04Nb
1150	27.5	3.4
1100	35.4	10.7
1050	41.0	17.0

2.1.2. Phase II: Validation Study Based on Experiment

To validate the theoretical predictions, deformation studies were conducted in the temperature range where rough rolling would be expected. The purpose of the experiments was to determine the extent of recrystallization of the austenite in the steels with different Nb levels and to compare these to the predicted values.

3. Materials and Methods

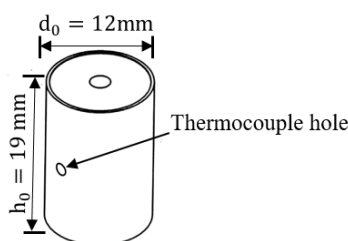
3.1. Experimental Materials

Laboratory heats of mass 45 Kg were vacuum melted and solidified in cast iron molds. The chemical compositions of the lab heats are listed in Table 2. These were hot rolled to 25 mm “slabs” in five passes with finishing temperature of 890 °C and air cooled to room temperature. The Nb-bearing heats were designated by L4, L8, H4 and H8, where the letter indicates the carbon level (i.e., L = 0.03 wt.% and H = 0.06 wt.%) and the number indicates Nb level (0 = Nb-free, 4 = 0.04 wt.% and 8 = 0.08 wt.%).

Table 2. Chemical composition of the experimental alloys in wt.%.

Alloy	C	Nb	Base
L0	0.032	-	1.88Mn-0.01P-0.002S-0.30Si-0.20Cu-0.20N-0.50Cr-0.10Mo-0.0145Ti-0.030Al-0.004N
L4	0.031	0.0429	
L8	0.029	0.0837	
H0	0.061	-	
H4	0.062	0.0413	
H8	0.059	0.07827	

From these slabs, 12 mm blanks were cut for producing cylinders for hot compression testing. Selected samples were machined to right cylindrical shapes of dimensions 12 mm (diameter) \times 19 mm (height), as shown in Figure 5. A thermocouple hole 1.6 mm in diameter and approximately 5 mm deep was drilled into the cylindrical samples to control and monitor the temperature.

**Figure 5.** Schematic of the cylinders used in this study for hot compression testing.

3.2. Studies of Grain Coarsening during Reheating

In order to quantify austenite grain size as a function of reheating temperature, grain coarsening experiments were conducted using isothermal holding at various reheating temperatures using cube samples having dimensions of 12 mm on a side. Prior to each soaking, samples were encapsulated in evacuated quartz tubes and filled with pure argon to minimize any oxidation effects. Samples were placed in a box furnace and were soaked for 60 min at different temperatures starting from 900 °C to 1300 °C in increments of 50 °C. Following that, the capsules were broken and the samples were quenched in water.

3.3. Hot Compression

To verify the predictions of the calculated Zener pinning forces, hot compression tests were performed in the temperature range where the roughing passes would be expected to occur; i.e., 1150–1000 °C. The right cylinders were reheated to 1200 °C for two minutes and then cooled to various temperatures for recrystallization studies. The deformations were applied using an MTS-458 unit designed for deformation under constant true strain rate conditions equipped with a radiation furnace and a temperature controller. Glass lubricant was used to suppress barreling in the multiple hit, axisymmetric hot compression tests. If the pinning forces were low in the rough rolling range, then repeated recrystallization would be expected with accompanying grain refinement. On the other hand, if the pinning forces were high, then complete recrystallization would not occur, and the grain size would stay large, reflecting the reheated grain size, and the grain shape would not be equiaxed. Figure 6 shows an example of the thermomechanical path used in the first series of samples to closely simulate roughing passes in a typical hot rolled plate. Two reduction levels of 15% and 25% were used in this study and the strain rate ($\dot{\epsilon}$) was set to be 10 s⁻¹ for all hot compression experiments.

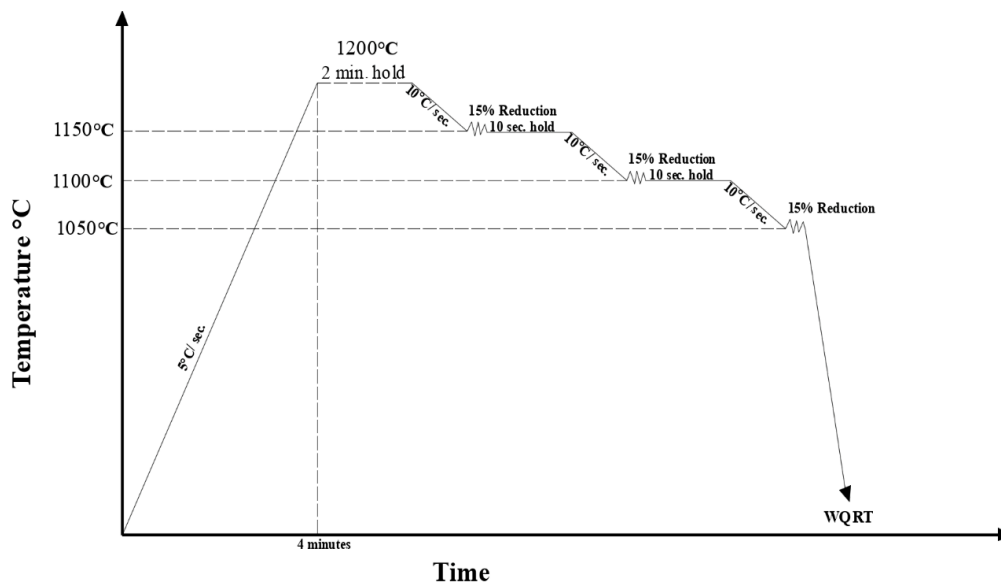


Figure 6. Thermomechanical schedules used in hot compression deformations with 15% reductions.

3.4. Characterization Methods

Samples from the as-received heats, grain coarsening studies and hot compression studies were analyzed using optical microscopy Nikon FX-35WA (Nikon Corp., Tokyo, Japan). Standard metallographic techniques were employed by mounting in Bakelite, grinding samples using waterproof abrasive silicon carbide papers gradually from grit 180 to 600 and polishing using alumina powders of 1 and 0.05 μm . The prior austenite grain boundaries were revealed using a special reagent consisting of 100 mL of saturated aqueous picric acid with the addition of 1 mL hydrochloric acid (HCL) and 10 g of sodium dodecylbenzene sulfonate as a wetting agent at 70 °C. The mean austenite grain sizes were measured using ImageJ (1.52a, National Institutes of Health, Bethesda, MD, USA), by manually outlining the austenite grains and calculating the equivalent grain diameter for each grain. From each sample, at least 400–500 grains were measured. Additionally, selected as-received samples were characterized using Vickers hardness tester LECO LM310AT (LECO Corp., St. Joseph, MI, USA). At least 5 Vickers hardness measurements with a load of 300 Kgf were taken from each direction in each of the selected samples. Further, in this study, EBSD Mapping was done in FEI Scios FIB/SEM Dual Beam (Thermo Fisher, Hillsboro, OR, USA) equipped with EDAX EBSD camera and TEAM software (V4.3, EDAX Inc., Mahwah, NJ, USA). Thin foils were examined under transmission electron microscope (TEM) using JEOL JEM2100F operating at an accelerated voltage of 200 kV.

4. Results and Discussion

4.1. As-Received Samples

Figure 7 shows optical micrographs of the air-cooled plates. It can be seen for the base alloys L0 and H0 in Figure 7a,b that the microstructures consisted mainly of polygonal ferrite (PF), and carbon-enriched constituents including acicular ferrite and/or martensite-austenite (MA) microconstituents. When the carbon is increased from 0.03 wt.% to 0.06 wt.%, the fraction of these carbon-enriched constituents was increased, as shown in Figure 7b. For the same cooling rate, the addition of Nb to the base alloys results in a complex microstructure, as can be observed in Figure 7c through Figure 7f. These complex microstructures consist of mainly acicular ferrite, MA and/or bainite. Another observation is that polygonal ferrite in the high Nb steels is suppressed significantly.

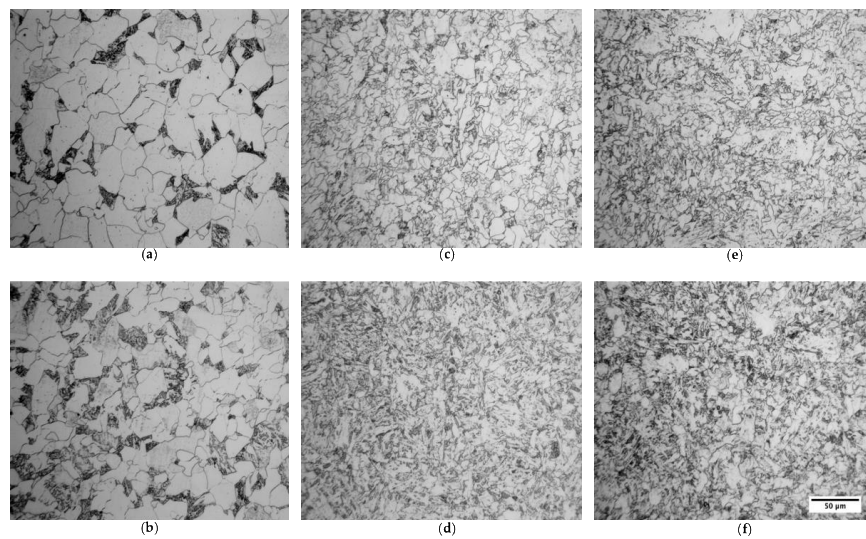


Figure 7. Optical metallographic microstructures of air-cooled samples: (a) L0, (b) H0, (c) L4, (d) H4, (e) L8 and (f) H8.

A TEM micrograph for H4 is shown in Figure 8. It is clearly evident that the steel contains a complex microstructure consisting of MA microconstituents and acicular ferrite. Additionally, a coarse, titanium-rich precipitate can be seen in the air cooled condition.

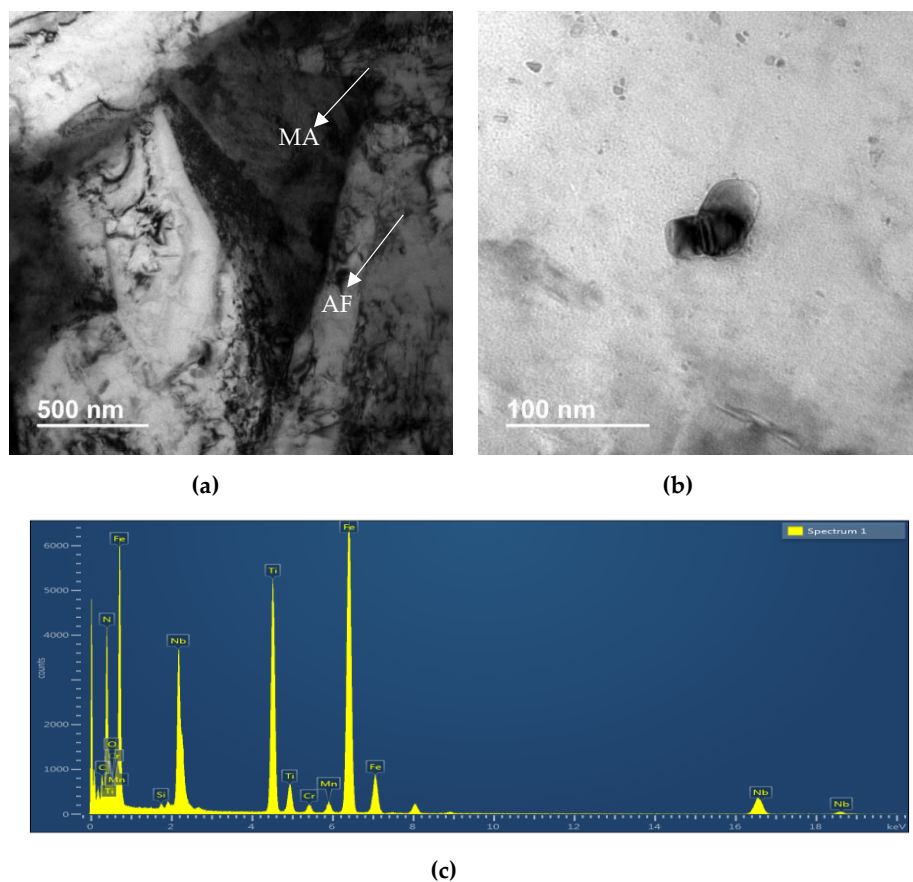


Figure 8. (a) Bright field image of H4 showing ferrite and carbon-enriched constituents. (b) Titanium-rich precipitate and the corresponding (c) EDS spectrum of the precipitate.

The hardness values of microstructures taken in the three normal directions, namely, normal direction (ND), rolling direction (RD) and transverse direction (TD), are shown in Figure 9. As expected, in general, as the carbon and/or niobium content increases, the hardness value increases, although for different reasons. For example, the higher Vicker's hardness number (VHN) values observed with increasing the carbon content appeared to be due to the fraction of carbon-enriched constituents. Although there is no clear evidence of which direction gives the highest hardness values in the investigated samples, the TD sample of H8 shows the highest value. It can be inferred from this that pancaking of the low carbon austenite in the roughing mill can occur easily in this direction, meaning that there is a higher tendency to nucleate hard carbon-enriched microconstituents in this direction.

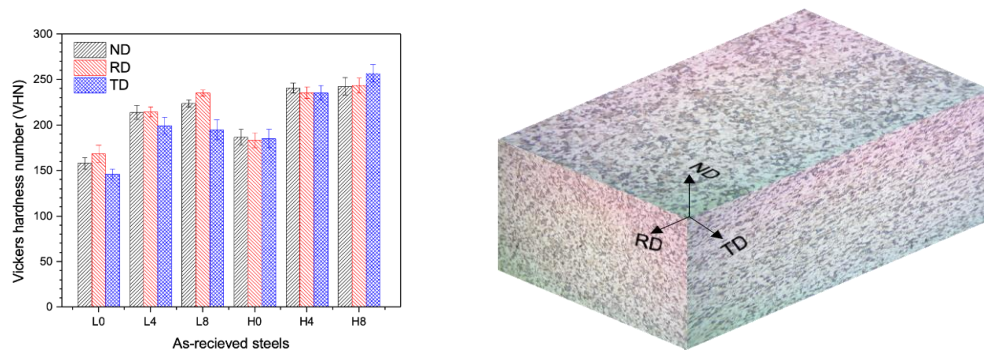


Figure 9. Vicker's hardness number (VHN) values of air-cooled samples in three orthonormal directions.

Another observation was made using EBSD mapping. Figure 10 depicts inverse pole figure data and misorientation angles of H0 and H8 taken from the transverse direction. For the same carbon level, there was a higher fraction of low angle grain boundaries (red boundaries) observed in H8 compared to H0, which is a typical characteristic of acicular ferrite.

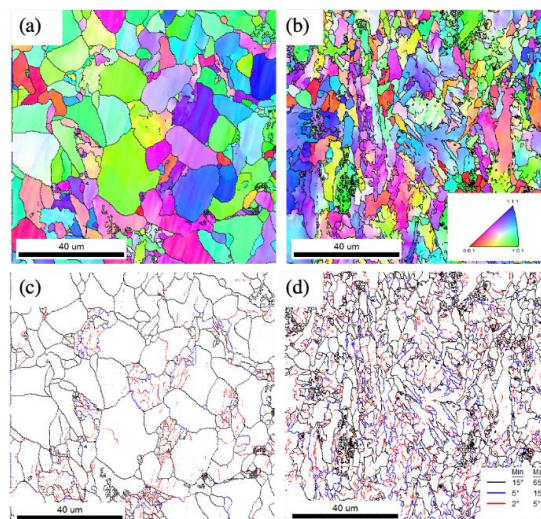


Figure 10. Inverse pole figure data and misorientation mapping of H0 (a,c) and H8 (b,d).

4.2. Coarsening of Prior Austenite Grain Size

Average austenite grain sizes as a function of reheating temperature for all six alloys are shown in Figure 11. Error bars represent 95% confidence intervals about the mean grain size. In general, austenite grain sizes increase with increasing the reheating temperatures. The Nb-bearing steels show a higher tendency for abnormal grain growth, a characteristic of microalloyed steels [25–27]. As an

example, a series of microstructures of L8 is depicted in Figure 12, and it can be seen that abnormal grain growth occurs at/ or close to 1100 °C.

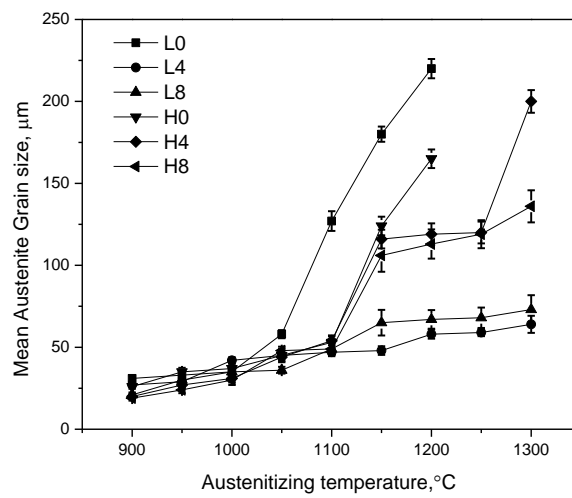


Figure 11. Mean austenite grain size as a function of reheating temperature.

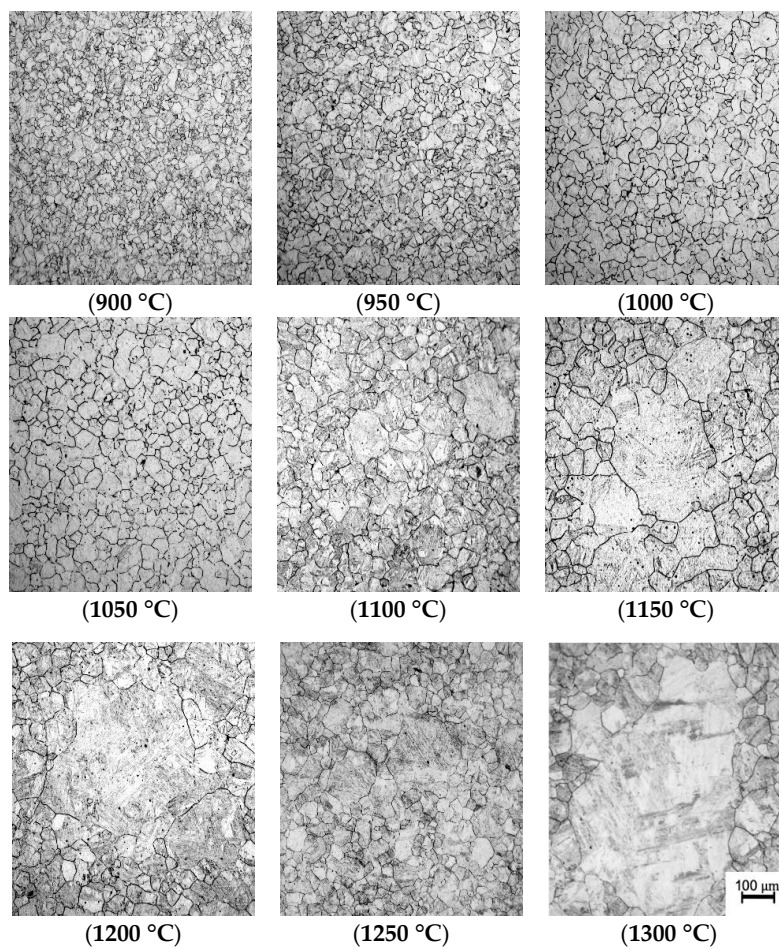


Figure 12. Light optical micrographs of prior austenite grains for steel L8 after soaking to the temperatures indicated.

4.3. Rough Rolling Simulations

The first series of samples was subjected to hot deformation of either two passes or three passes in the temperature range between 1150 and 1050 °C, where each pass was under 15%. Figure 13a–c shows samples subjected to two-pass deformation at 1150 °C and 1100 °C of H4, H8 and L8, respectively. Complete recrystallization is observed in all three samples under two passes and three passes. It is expected from solubility products that the fraction of NbC or NbCN in H8 during cooling is higher than those in H4 and L8. For the three pass microstructures, it can be seen in Figure 13d–f, that the average austenite grain sizes are reduced, and the highest reduction in grain size was observed in L8 samples during hot deformation. Figure 14 summarizes the average austenite grain sizes of steels H4, H8 and L8.

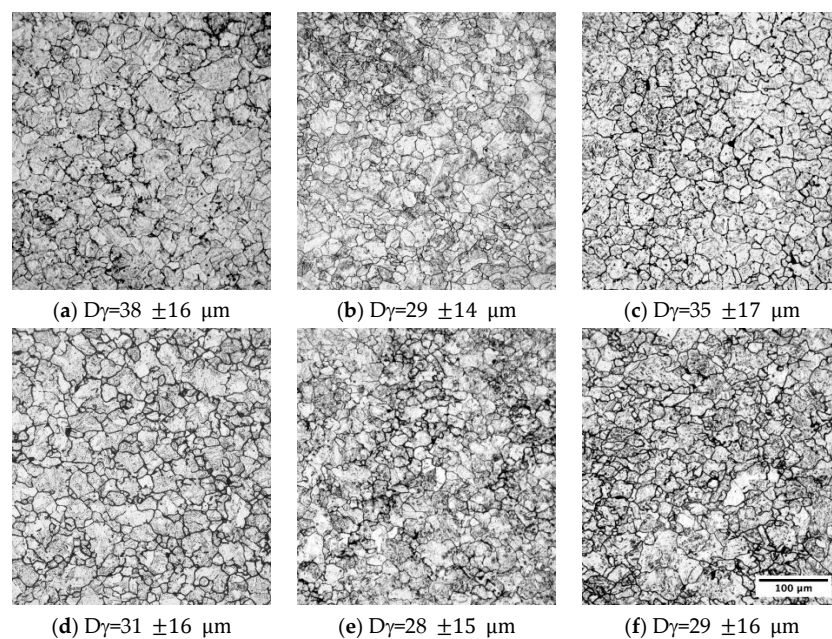


Figure 13. Two-pass reduction of 15% at 1150 and 1100 °C for (a) H4, (b) H8 and (c) L8; three pass reduction at 1150, 1100, and 1050 °C for (d) H4, (e) H8 and (f) L8.

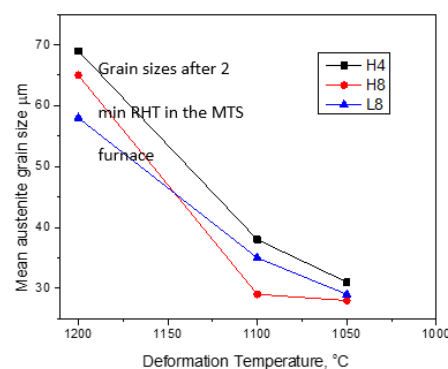


Figure 14. Mean austenite grain size after two passes with 15% reduction/pass at the respective deformation temperature; each sample was quenched, and prior austenite grain size was analyzed.

The second series of samples was subjected to three passes under 25% reduction in each pass. The micrographs of these samples are shown in Figure 15. It is evident from these micrographs that pancaking of austenite did not occur, even at 1050 °C. However, a non-uniform austenite grain distribution can be observed at temperatures at/or below 1050 °C in the high Nb steels. This leads to a mixture of recrystallized and unrecrystallized austenite grains (i.e., duplex austenite grains) in

the roughing stage of plate steels. To demonstrate this idea, the L8 sample was reheated at 1200 °C for two minutes and subjected to three 25% passes, but the last pass was done at 1030 °C, which is near the end of the roughing passes. The interpass time was set to be 15 s after each pass in order to see whether complete static recrystallization could be observed. Figure 16 shows the prior austenite grain size of L8 subjected to the previously mentioned schedule, and the fraction of unrecrystallized grains was measured to be 15% based on the non-circularity of the grains. This may show that the recrystallization stop temperature is close to the range of 1030–1000 °C.

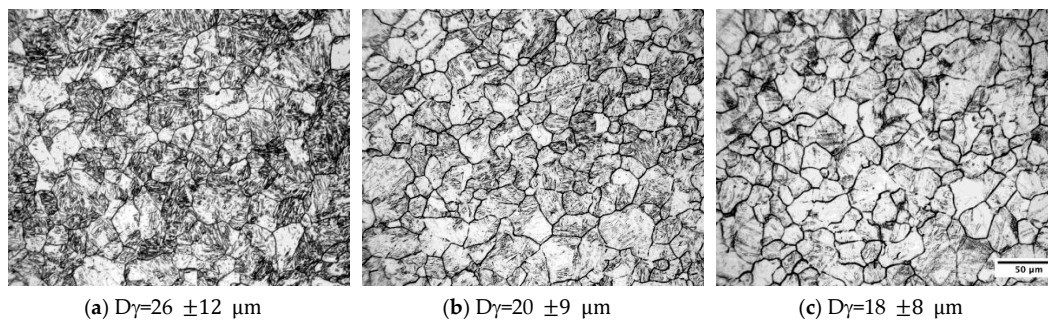


Figure 15. Three-pass reduction of 25% each at 1150, 1100 and 1050 °C for (a) H4, (b) H8 and (c) L8.

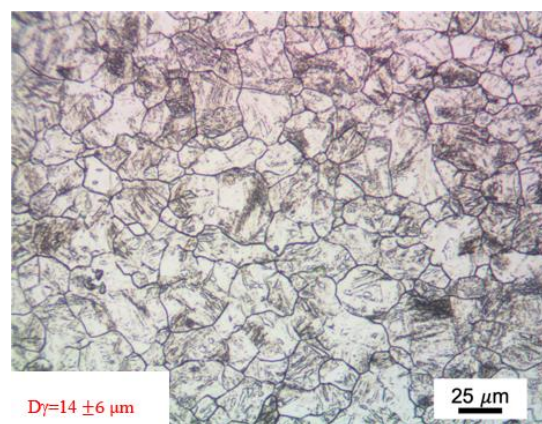


Figure 16. L8 subjected to three passes of 25% each at 1150, 1100 and 1030 °C; the interpass time was 15 s. The compression axis is vertical.

This also indicates that the NbC pinning force is large enough to retard recrystallization in the roughing stage. The resulting duplex microstructure at the end of the roughing passes and can deteriorate strength and toughness in the final product.

It is immediately apparent that higher pinning forces of NbC on austenite grain boundaries will increase the $T_{5\%}$ to higher temperatures, which may lead to a duplex microstructure at the end of rough rolling. Thus, it is necessary to choose Nb levels perhaps well below 0.1 wt.% to have uniform austenite grain sizes at the end of roughing rolling. This is true for both plate mills and thin slab casting mills, where the few, if any, roughing passes or the early finishing passes acting as roughing passes occur at temperatures above 950 °C, thereby eliminating or reducing the possibility of grain refinement before experiencing the low temperature finishing passes.

While further investigation is needed to confirm the effects of C and Nb levels on grain coarsening and recrystallization behaviors based on precipitate analyses, this study draws attention to the necessity to keep Nb levels optimum to produce a uniformly refined austenite grain size during the rough rolling of plate steels. Additionally, the study of the interaction between precipitation and recrystallization in the finishing passes of hot rolled plates needs to be considered in future studies.

5. Conclusions

From the present investigation, the following conclusions can be drawn:

For the same thermomechanical processing schedule, the as-received samples show different microstructures, depending on carbon and niobium contents. The Nb-free alloys mainly consist of polygonal ferrite and some carbon enriched constituents, while the Nb-bearing alloys exhibit acicular microstructures with significantly reduced amounts of polygonal ferrite.

Based on equilibrium thermodynamic relations, it appears that strain-induced NbC can precipitate in the roughing temperature range in high Nb steels.

Depending of the amount of strain, the suppression of some recrystallized austenite grains would be expected to cause duplex grain structures, which is believed to be responsible for inferior mechanical properties.

Author Contributions: Conceptualization, A.J.D.; methodology, A.J.D. and R.A.A.; validation, A.J.D. and R.A.A.; formal analysis, R.A.A. and A.J.D.; writing—original draft preparation, R.A.A.; writing—review and editing, A.J.D.; supervision, A.J.D.; project administration, A.J.D.; funding acquisition, A.J.D. All authors have read and agreed to the published version of the manuscript.

Funding: The Basic Metals Processing Institute, Department of Mechanical Engineering and Materials Science, University of Pittsburgh thanks its industrial sponsors for partially funding this study. In addition, the United States Steel Corporation (U.S. Steel) should be thanked for providing the experimental materials and processing. Finally, one of the authors (Almatani), was supported by a scholarship from King Abdulaziz City for Science and Technology (KACST), Saudi Arabia.

Acknowledgments: The authors would like to thank the Basic Metals Processing Institute, Department of Mechanical Engineering and Materials Science, University of Pittsburgh and its industrial sponsors for partially funding this study. In addition, the United States Steel Corporation (U.S. Steel) should be thanked for providing the experimental materials and processing. Finally, one of the authors (Almatani), was supported by a scholarship from King Abdulaziz City for Science and Technology (KACST), Saudi Arabia.

Conflicts of Interest: The authors declare no conflict of interest.

References

1. Beiser, C.A. The Effect of Small Columbium Additions to semi-killed Medium-Carbon Steels. ASM Preprint No. 138. In Proceedings of the Regional Technical Meeting, Buffalo, NY, USA, 17–19 August 1959.
2. Stuart, H. Niobium-Proceedings of the International Symposium. Metallurgical Society of AIME: Warrendale, PA, USA, 1984.
3. Hansen, S.; Vander Sande, J.; Cohen, M. Niobium carbonitride precipitation and austenite recrystallization in hot-rolled microalloyed steels. *Metall. Trans. A* **1980**, *11*, 387–402. [[CrossRef](#)]
4. Cuddy, L. Microstructures developed during thermomechanical treatment of HSLA steels. *Metall. Trans. A* **1981**, *12*, 1313–1320. [[CrossRef](#)]
5. Sobral, M.; Mei, P.; Kestenbach, H.-J. Effect of carbonitride particles formed in austenite on the strength of microalloyed steels. *Mater. Sci. Eng. A* **2004**, *367*, 317–321. [[CrossRef](#)]
6. Vervynckt, S.; Verbeken, K.; Lopez, B.; Jonas, J.J. Modern HSLA steels and role of non-recrystallisation temperature. *Int. Mater. Rev.* **2012**, *57*, 187–207. [[CrossRef](#)]
7. Priestner, R.; Hodgson, P. Ferrite grain coarsening during transformation of thermomechanically processed C–Mn–Nb austenite. *Mater. Sci. Technol.* **1992**, *8*, 849–854. [[CrossRef](#)]
8. Miao, C.; Shang, C.; Zurob, H.; Zhang, G.; Subramanian, S. Recrystallization, precipitation behaviors, and refinement of austenite grains in high Mn, high Nb steel. *Metall. Mater. Trans. A* **2012**, *43*, 665–676. [[CrossRef](#)]
9. Iron and Steel Institute of Japan. *Proceedings of the Conference Thermec 88, Tokyo, Japan 1988*; Iron and Steel Institute of Japan: Tokyo, Japan, 1988; Volume 1, pp. 330–336.
10. Tanaka, T. Controlled rolling of steel plate and strip. *Int. Met. Rev.* **1981**, *26*, 185–212. [[CrossRef](#)]
11. Shanmugam, S.; Misra, R.D.K.; Mannering, T.; Panda, D.; Jansto, S.G. Impact toughness and microstructure relationship in niobium-and vanadium-microalloyed steels processed with varied cooling rates to similar yield strength. *Mater. Sci. Eng. A* **2006**, *437*, 436–445. [[CrossRef](#)]
12. Palmiere, E.J. Suppression of Recrystallization during the Hot Deformation of Microalloyed Austenite. Ph.D. Thesis, University of Pittsburgh, Pittsburgh, PA, USA, 1991.

13. Watanabe, H.; Smith, Y.; Pehlke, R. Precipitation kinetics of niobium carbonitride in austenite of high-strength low-alloy steels. In *The Hot Deformation of Austenite*; TMS-AIME: New York, NY, USA, 1977; pp. 140–168.
14. Rajinikanth, V.; Kumar, T.; Mahato, B.; Chowdhury, S.G.; Sangal, S. Effect of Strain-Induced Precipitation on the Austenite Non-recrystallization (Tnr) Behavior of a High Niobium Microalloyed Steel. *Metall. Mater. Trans. A* **2019**, *50*, 5816–5838. [[CrossRef](#)]
15. Palmiere, E.J.; Garcia, C.I.; DeArdo, A.J. The influence of niobium supersaturation in austenite on the static recrystallization behavior of low carbon microalloyed steels. *Metall. Mater. Trans. A* **1996**, *27*, 951–960. [[CrossRef](#)]
16. Koo, J.Y.; Luton, M.J.; Bangaru, N.V.; Petkovic, R.A.; Fairchild, D.P.; Petersen, C.W. Metallurgical design of ultra high-strength steels for gas pipelines. *Int. J. Offshore Pol. Eng.* **2004**, *14*, 2–10.
17. Graf, M.K.; Hillenbrand, H.G.; Peters, P. *Accelerated Cooling of Steel*; TMS-AIME: Warrendale, PA, USA, 1986; pp. 165–179.
18. Cuddy, L. The Effect of Microalloy Concentration on the Recrystallisation of Austenite During Hot Deformation. In *Thermomechanical Processing of Microalloyed Austenite*; AIME: Pittsburgh, PA, USA, 1981; pp. 129–140.
19. Kozasu, I.; Ouchi, C.; Sampei, T.; Okita, T. Hot rolling as a high-temperature thermo-mechanical process. In *Proceedings of the Conference on Microalloying 75*; Union Carbide Corp.: New York, NY, USA, 1977; pp. 120–135.
20. Palmiere, E.J.; Garcia, C.I.; DeArdo, A.J. Compositional and microstructural changes which attend reheating and grain coarsening in steels containing niobium. *Metall. Mater. Trans. A* **1994**, *25*, 277–286. [[CrossRef](#)]
21. Murr, L.E. *Interfacial Phenomena in Metals and Alloys*; Advanced Book Program, Reading, Mass; Addison-Wesley Pub. Co.: New York, MA, USA, 1974.
22. Danieli, C. *Start up Model for a Five Meter Plate Mill*; Private Communication: SpA. Buttrio (UD), Italy, 2010.
23. Gladman, T. On the theory of the effect of precipitate particles on grain growth in metals. *Proc. R. Soc. Lond. A* **1966**, *294*, 298–309.
24. Palmiere, E.J.; Garcia, C.I.; DeArdo, A.J. The influence of niobium supersaturation in austenite on the static recrystallization behavior of low carbon microalloyed steels. *Metall. Mater. Trans. A* **1996**, *27*, 951–960. [[CrossRef](#)]
25. Kwon, O.; DeArdo, A.J. Interactions between recrystallization and precipitation in hot-deformed microalloyed steels. *Acta Metall. Mater.* **1991**, *39*, 529–538. [[CrossRef](#)]
26. Cuddy, L.; Raley, J. Austenite grain coarsening in microalloyed steels. *Metall. Trans. A* **1983**, *14*, 1989–1995. [[CrossRef](#)]
27. Fernández, J.; Illescas, S.; Guilemany, J.M. Effect of microalloying elements on the austenitic grain growth in a low carbon HSLA steel. *Mater. Lett.* **2007**, *61*, 2389–2392. [[CrossRef](#)]

